

***Ab initio* study on the mechanism of $C_2H_2^+ + NH_3$ reaction: Efficient charge transfer and proton transfer processes competing with stable complex formation**

Qiang Cui and Keiji Morokuma

Cherry L. Emerson Center for Scientific Computation and Department of Chemistry, Emory University, Atlanta, Georgia 30322

(Received 14 November 1997; accepted 4 December 1997)

High level *ab initio* calculations have been performed to investigate the mechanism of the ion-molecule reaction $NH_3 + C_2H_2^+$. Three channels, covalent complex formation (CC), proton transfer (PT), and charge transfer (CT) have been studied. Among the two pathways found for the PT channel, one leads the reactants $NH_3 + C_2H_2^+$ to $NH_4^+ + C_2H(^2\Pi)$ through a moderately bound complex without any barrier, and the other leads $NH_3 + C_2H_2^+$ to the H-atom transferred products $NH_4^+ + C_2H(^2\Sigma^+)$ with a modest barrier. These findings support the fast "stripping" mechanism proposed by Anderson *et al.* As to the CC channel, several isomers of $C_2H_5N^+$ and the isomerization transition states have been located. No significant barrier relative to the reactants has been found on either the ground or the $^2A''$ excited state. To rationalize the experimental fact that no CC channel products have been observed, it is argued that the reactants $NH_3 + C_2H_2^+$ correlate adiabatically to excited states of covalent $C_2H_5N^+$ species, whose formation requires significant alternation of the $C_2H_2^+$ geometry and electronic structure. Therefore, the system is most likely to follow the PT or the CT channel instead of visiting the CC channel. For the CT channel, limited potential energy surface scans of the three electronic states ($1,2^2A' + ^2A''$) indicate that CT at different approach angles or between electronic states of different symmetries ($A' \rightarrow A', A'' \rightarrow A'$) may produce final products of different characteristics, and might account for the two pathways proposed by Anderson *et al.* © 1998 American Institute of Physics. [S0021-9606(98)02510-0]

I. INTRODUCTION

The potential energy surfaces for polyatomic systems are usually very complicated, and often consist of intermediate complexes of very different chemical natures. These complexes may or may not be separated by large barriers depending on the type of reorganization of atomic and electronic configurations required. Typical examples are the $[H,N,C,O]$ and $[H,N,C,O]^+$ systems, where a large number of intermediates and transition states connecting them at different energetic ranges have been found.¹ In such cases, a fundamental question that often arises is how much configuration space the molecule visits with certain initial conditions. Can one sample a particular part of the configuration space selectively by somehow altering the initial conditions? In the cases where a large barrier exists between different regions, it is clear that some special technique has to be employed to sample the isolated territory on the potential energy surface. In the past decade or so, exciting laser techniques such as photodetachment have been well developed and applied to many systems to probe particular parts of the potential energy surface. In some molecular systems, however, a certain part of configuration space is rarely visited, not due to high barriers around them but because of the existence of some *dynamic bottleneck*. The system of $C_2H_2^+ + NH_3$, which was recently studied by Anderson *et al.*,² belongs to this class.

In the experiment, the product ion recoil velocity distributions from the reaction of $C_2H_2^+ + ND_3$ have been ana-

lyzed. There are three product channels observed over a wide range of the center-of-mass (c.m.) collision energy range from 0.1 to 5 eV: charge transfer (CT, ND_3^+) CT with H/D exchange (ND_2H^+) and proton transfer (PT, ND_3H^+). The ratio of the CT and PT channels has been estimated to be 80:20 at low collision energy, and the charge-transfer channel becomes dominant as the collision energy increases. Surprisingly, no evidence for the formation of the stable $C_2H_5N^+$ intermediates has been observed, despite the existence of several strongly bound isomers. The H-abstraction channel, which was dominant at high collision energy for the isoelectronic system of $C_2H_2^+ + CH_4$,³ to produce $C_2H_3^+ + NH_2$, was not observed either. It is not surprising that the charge-transfer and proton transfer channels become open for the NH_3 system, compared to the CH_4 system, due to thermodynamic reasons. However, the thermodynamic properties for the complex channel and the H-abstraction channel are qualitatively similar for both systems. Therefore, it is really intriguing why these channels have been observed experimentally for $C_2H_2^+ + CH_4$ but not for $C_2H_2^+ + NH_3$ over a wide range of collision energy.

The velocity distributions of the PT channel products are strongly backward peaked, even at low collision energy. The portion of the energy that was partitioned into product recoil has been estimated to be rather large at any collision energy, much larger than expected for statistical distribution into all the degrees of freedom. All these observations suggest that

PT is a direct channel with a proton-stripping mechanism.

As to the CT channel, two different mechanisms seem to exist. At low collision energy, the recoil velocity of the product ND_3^+ and ND_2H^+ are very similar and forward-backward symmetric. This implies that the charge transfer takes place through a complex mediated mechanism, which has a lifetime longer than ~ 1 psec. This complex seems to be weakly bound, as suggested by the limited H/D scrambling observed experimentally. At higher collision energy, the recoil velocity distribution shifts backward in the c.m. frame. Thus at high collision energy, the charge is transferred with little momentum transfer, leaving the ND_3^+ with near zero laboratory velocity, which is consistent with a long-range electron hopping mechanism. However, it was puzzling to notice that the velocity distribution of ND_2H^+ is also very similar to that of ND_3^+ at high collision energy.

Finally, the effect of vibrational excitation in the reactant C_2H_2^+ on the reaction has also been examined, as in the study of $\text{C}_2\text{H}_2^+ + \text{CH}_4$, where a large effect has been observed.³ The effect is much smaller in the present system, albeit very mode-specific. In the PT channel, the reaction is enhanced by C_2H_2^+ bending and inhibited by the CC stretch over the entire collision energy range studied experimentally. In the CT channel, both CC stretch and bending in C_2H_2^+ inhibit the reaction at high collision energy. At low collision energy, the reaction is inhibited by $\sim 25\%$ by the CC stretch, but enhanced by $\sim 30\%$ by the HCC bending in C_2H_2^+ . All these suggest a reaction mechanism where the C_2H_2^+ vibration influences the probability of a favorable reactant geometry arrangement, while the branching between product channels is determined later in the collision by factors not strongly dependent on the reactant vibration. However, the origin of the mode-specificity observed remains unclear.

To see if theoretical calculations can shed some light on the issues arising from the experimental work of Anderson *et al.*,² we have carried out *ab initio* studies to investigate at first the structures and energetics of important intermediates and transition states involved in the system. In the past, only limited calculations on the covalently bound complexes of the $[\text{NH}_3 \cdot \text{C}_2\text{H}_2]^+$ system have been carried out,⁴ and very little is known about the part of the potential surface related to the CT and PT channels.

In the current work, we have studied the global potential energy surface, in the hope of unraveling the relationship between the potential energy surface and the reaction dynamics. In the present paper, we first discuss briefly the methods we have employed in the study. The results from our calculation will be presented in Sec. III, and the mechanism of the reaction will be discussed based on these results in conjunction with the experimental findings just summarized above. Finally, we make a few conclusions in Sec. IV.

II. COMPUTATIONAL METHOD

The structures of the intermediates and transition states have been obtained at the B3PW91^{5,6}/6-311G(*d,p*)⁷ level. The more popular method B3LYP was not employed here because in some preliminary calculations we found that it gave not as satisfactory results for C_2H and C_2H_3^+ as the

B3PW91 functional. For instance, the B3LYP/6-311G(*d,p*) method predicted a nonlinear equilibrium structure for the $^2\text{IC}_2\text{H}$, whereas the B3PW91/6-311G(*d,p*) calculation gave a linear geometry which is more consistent with the experimental observations and previous theoretical treatments. The energetics of these critical structures have been further improved with the G2M(RCC)⁸ method. The G2M(RCC) method uses the RCCSD(T)/6-311G(*d,p*) method as the highest correlation level and calculates basis set corrections mainly at the MP4 level. The method is very accurate, reproducing the atomization energy for the G2 test set with an average absolute deviation of 1.15 kcal/mol and is applicable reliably to open-shell systems, such as in the present case. Since more than one electronic state is involved in both the CT and the PT channels, we have also used the CASSCF⁹/6-31G(*d,p*)¹⁰ method to study the part of the potential energy surface where surface crossing is expected. The active space used in the CASSCF calculations depends on the region of the surface studied, and will be discussed in more detail in Sec. III. We have employed similar methods in the study of $\text{C}_2\text{H}_2^+ + \text{CH}_4$.¹¹ The DFT and G2M calculations have been carried out with the GAUSSIAN94 package,¹² and CASSCF calculations were carried out with the MOLPRO96 package.¹³

III. AB INITIO CALCULATIONS

Energetics of the intermediates and transition states involved in the reaction are summarized in Table I. The geometries of these structures are shown in Figs. 1 and 4. A schematic global reaction profile is presented in Fig. 2. Scans of potential energy surfaces related to the PT and CT channels are presented in Figs. 3 and 5, respectively.

In the present *ab initio* calculations, three reaction channels are distinguished, the proton transfer (PT) channel, the covalent complex formation (CC) channel, and the charge-transfer (CT) channel. We shall discuss the potential energy surface and the detailed reaction mechanism for these channels separately in the following sections. The intermediates and transition states are labeled according to the channel, e.g., **CC_2** and **PT_TS1** stand for an intermediate in the covalent complex formation channel and a transition state in the proton transfer channel, respectively. Before going into the discussion, however, we first notice that several properties of the reactants and products such as adiabatic ionization potentials of NH_3 (10.20 vs 10.18 eV exper.) and C_2H_2 (11.42 vs 11.42 eV exper.), proton affinity of NH_3 (8.77 vs 8.78 eV exper.), and bond dissociation energy of C_2H_2 (5.78 vs 5.72 eV exper.) and NH_3 (4.60 vs 4.68 eV exper.), as shown in Table I, are in excellent agreement with experimental values. This provides some criteria about the accuracy of the method G2M(RCC)//B3PW91/6-311G(*d,p*) employed in the present study.

A. Proton transfer channel (PT)

In the experiment, the detection of velocity distribution of NH_4^+ (or actually its isotopomer ND_3H^+) indicates that the proton transfer channel follows a direct stripping mechanism at even low collision energy. No examination of the final

TABLE I. Energetics of intermediates, transition states in the reaction of $\text{NH}_3 + \text{C}_2\text{H}_2^+$.^a

Structure	State	B3PW91/I	PMP4/I	UCCSD(T)/I	PMP4/II	PMP4/III	MP2/IV	G2M	G2M+ZPE
NH_3	1A_1	-56.554 57	-56.428 03	-56.428 31	-56.434 32	-56.456 55	-56.450 59	---	---
C_2H_2^+	$^2\Pi_g$	-76.903 66	-76.729 98	-76.731 15	-76.730 87	-76.763 91	-76.734 90	0.00	0.00
$\text{NH}_2 + \text{C}_2\text{H}_3^+$		0.36	0.29	0.32	0.34	0.26	0.36	0.34	0.14
$\text{C}_2\text{H}_2 + \text{NH}_3^+$		-1.25	-1.44	-1.39	-1.31	-1.43	-1.28	-1.20	-1.22
$\text{C}_2\text{H} + \text{NH}_4^+$		-0.97	-1.13	-1.12	-0.99	-1.08	-0.52	-0.91	-0.80
$D(\text{NH}_2\text{-H})^b$			4.73	4.74	4.77	4.79	4.96	5.02	4.60
I.P.(NH_3) ^b		-9.98	-9.70	-9.70	-9.86	-9.89	-10.20	-10.25	-10.20
I.P.(C_2H_2) ^b		-11.24	-11.14	-11.09	-11.16	-11.31	-11.48	-11.45	-11.42
$D(\text{C}_2\text{H-H})^b$			5.88	5.85	5.88	5.97	6.49	6.12	5.78
$\text{PA}(\text{NH}_3)^b$		-9.43	-9.46	-9.47	-9.31	-9.34	-9.13	-9.18	-8.77
PT_1	2E	-1.74	-1.74	-1.73	-1.60	-1.72	-1.48	-1.55	-1.41
PT_TS1	2A_1	-0.70	-0.71	-0.61	-0.56	-0.71	-0.03	-0.44	-0.45
PT_TS2	$^2A'$	-1.43	-1.27	-1.26	-1.13	-1.26	-1.08	-1.08	-1.11
CC_1_cis	$^2A'$	-3.43	-3.31	-3.28	-3.16	-3.34	-3.01	-3.16	-2.93
CC_1_trans	$^2A'$	-3.52	-3.40	-3.39	-3.26	-3.42	-3.10	-3.26	-3.01
CC_1_ex	$^2A''$	-1.07	-0.89	-0.94	-0.77	-0.88	-0.69	-0.81	-0.61
CC_2	$^2A''$	-5.11	4.88	-4.81	-4.73	-4.95	-4.73	-4.73	4.49
CC_2_ex	$^2A''$	-2.93	-2.60	-2.59	-2.50	-2.67	-2.61	-2.55	-2.15
CC_2_ex2	$^2A''$							-0.30 ^c	
CC_3	$^2A'$	-3.74	-3.52	-3.51	-3.38	-3.57	-3.25	-3.40	-3.28
CC_3_ex	$^2A''$	-2.19	-1.80	-1.83	-1.67	-1.84	-1.60	-1.75	-1.60
CC_4	$^2A'$	-4.27	-4.00	-3.97	-3.85	-4.05	-3.92	-3.86	-3.68
CC_4_ex	$^2A''$	-0.25	-0.01	-0.07	0.12	0.03	0.36	0.10	0.14
CC_TS_ex	$^2A''$	-0.49	-0.13	-0.16	-0.01	-0.17	0.05	-0.05	0.05
CC_TS_12	$^2A'$	-1.74	-1.53	-1.46	-1.39	-1.59	-1.06	-1.36	-1.31
CC_TS_12_ex	$^2A''$	-0.54	-0.21	-0.22	-0.07	-0.23	-0.06	-0.09	-0.02
CC_TS_23	$^2A'$	-2.16	-1.96	-1.86	-1.81	-2.02	-1.60	-1.76	-1.72
CC_TS_24	2A	-2.76	-2.32	-2.31	-2.19	-2.42	-2.31	-2.28	-2.18
CC_TS_34	$^2A'$	-1.87	-1.59	-1.51	-1.46	-1.70	-1.54	-1.46	-1.49

^aOptimized at the B3PW91/6-311G(*d,p*) level. Total energies in hartree are shown in italics for the reactants, and relative energetics respective to $\text{NH}_3 + \text{C}_2\text{H}_2^+$ in eV are shown for the other structures. Basis notations are: I-6-311G(*d,p*), II-6-311+G(*d,p*), III-6-311G(2*df,p*), IV-6-311+G(3*df,2p*). No ZPE included in the relative energetics unless specified. ZPEs are calculated at B3PW91/6-311G(*d,p*) level.

^bThe experimental values are: $D(\text{NH}_2\text{-H})$ 4.68, I.P.(NH_3) 10.18, I.P.(C_2H_2) 11.40, $D(\text{C}_2\text{H-H})$ 5.72, $\text{PA}(\text{NH}_3)$: 8.78.

^cThis value was obtained by adding the 4.44 eV adiabatic excitation energy (without ZPE), calculated at the EOM-CCSD/6-311G(*d,p*)/EOM-CCSD/6-31G(*d,p*), level to the G2M (without ZPE) energy of **CC_2**.

electronic state of the other product C_2H has been carried out. According to the following theoretical analysis, we notice that two PT channels actually exist, producing C_2H in different electronic states.

First of all, we notice that for both the reactants and products of the PT channel, close lying electronic states exist. For the reactants, $\text{C}_2\text{H}_2^+(^2\Pi) + \text{NH}_3$ is doubly degenerate, while the low lying $\text{C}_2\text{H}_2 + \text{NH}_3^+$ state has no spatial degeneracy. For the products, as shown in Fig. 2, $\text{C}_2\text{H}(^2\Sigma^+) + \text{NH}_4^+$ is the lowest asymptote, with the upper dissociation asymptote $\text{C}_2\text{H}(^2\Pi) + \text{NH}_4^+$ being only 0.50 eV higher in energy, and also lower than the reactants of $\text{C}_2\text{H}_2^+ + \text{NH}_3$. If the reaction proceeds with perfect linear N-C-C framework, which might just be the minimum energy path considering the favorable geometry arrangement. C_{3v} symmetry is then maintained during the reaction. In C_{3v} , both $\text{C}_2\text{H}_2^+(^2\Pi) + \text{NH}_3$ and $\text{C}_2\text{H}(^2\Pi) + \text{NH}_4^+$ fall into the doubly degenerate 2E symmetry and are directly correlated, which will be denoted as the PT1 channel. On the other hand, $\text{C}_2\text{H}_2 + \text{NH}_3^+$ and $\text{C}_2\text{H}(^2\Sigma^+) + \text{NH}_4^+$ both fall into the 2A_1 symmetry, and are directly correlated, which will be denoted as the PT2 channel, although it is actually an H atom that has been transferred.

During the electronic structure calculations, we employed C_s symmetry, since most *ab initio* programs cannot handle non-Abelian point group with degeneracy. For each structure, we examine both the A' and A'' states, and determine if the electronic state is 2E or 2A_1 . Interestingly, we have found that two PT channels have a rather different general shape of potential energy surfaces. The PT1 channel in the 2E symmetry does not involve any entrance or exit barrier, and proceeds through an intermediate complex **PT_1** in Fig. 1, which resembles the products $\text{C}_2\text{H}(^2\Pi) + \text{NH}_4^+$. The PT2 channel, on the other hand, proceeds through a transition state **PT_TS1**, also in Fig. 1,¹ and no intermediate is involved. It is interesting to note that although the 2E state in C_{3v} is subject to Jahn-Teller distortion in general, the effect is evidently very small in the case of **PT_1**. Although the calculation is carried out in C_{3v} the A' and A'' states are nearly degenerate, and all the vibrational frequencies are real. This is not unexpected because the structure of **PT_1** is very productlike, in which the $\text{C}_2\text{H}(^2\Pi)$ state is well known to be linear both experimentally¹⁴ and theoretically.¹⁵ The existence of the barrier in the PT2 channel is not surprising either, since unlike proton transfer processes, most H-atom transfer reactions proceed with barriers. At the

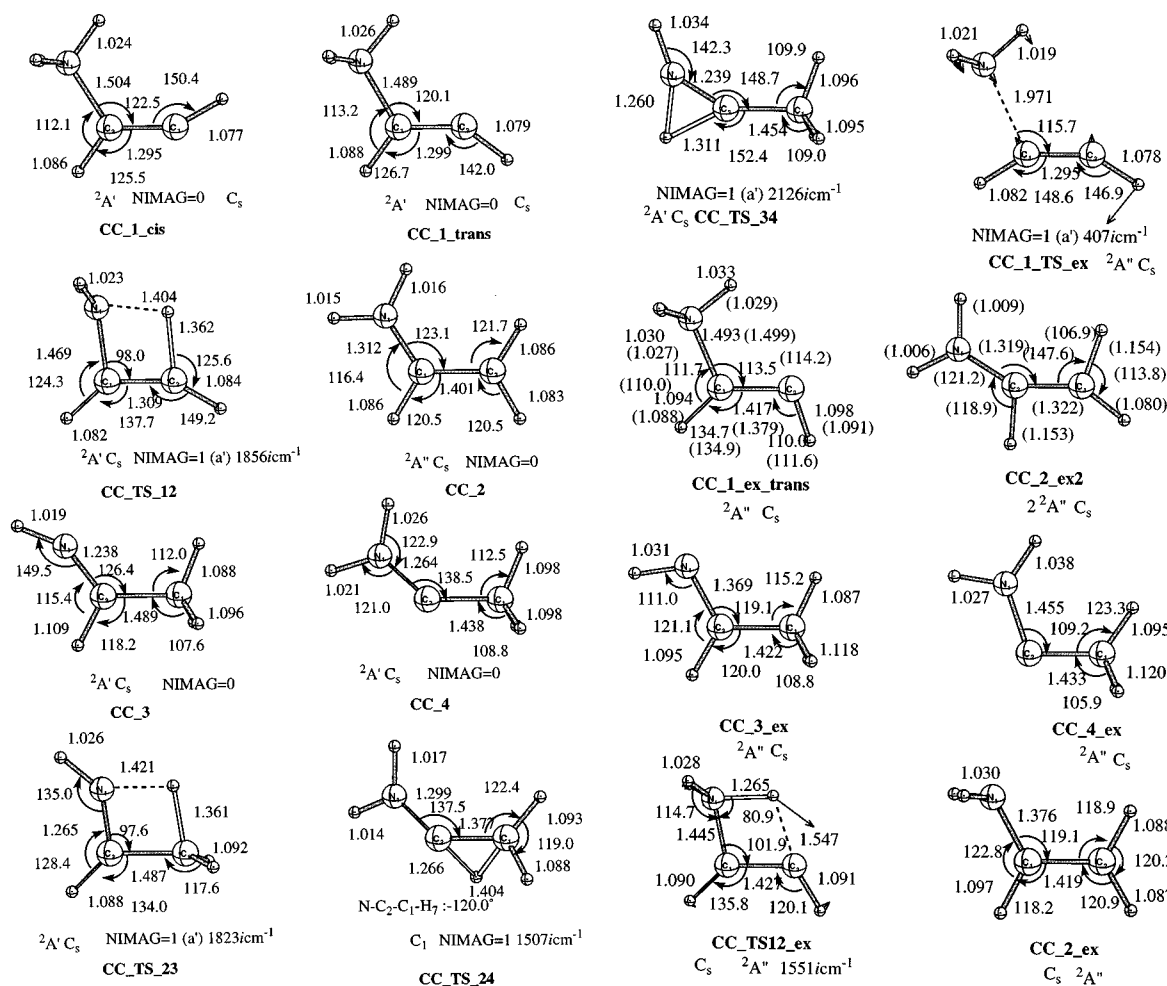


FIG. 4. Geometries (in Å and deg) of intermediates and transition states involved in the covalent complex formation channel of the reaction of $\text{NH}_3 + \text{C}_2\text{H}_2^+$ optimized at the B3PW91/6-311G(*d,p*) level.

diates in the PT2 channel have been verified by the CASSCF calculation. However, a shallow entrance complex seems to exist according to Fig. 3(b). It turned out that this well on the 2A_1 surface comes from the fact that the fixed NH_3 geometry used in the scan is too pyramidal, therefore the reactants in the PT2 channel, $\text{NH}_3 + \text{C}_2\text{H}_2$, are destabilized too much. If one chooses a less pyramidal configuration for NH_3 , the well on the surface disappears. Indeed, optimization for the 2A_1 state on the CASSCF level simply leads to the separated NH_3^+ and C_2H_2 .

What happens if the molecule bends and breaks the C_{3v} symmetry? An immediate answer is that the ${}^2A''$ state retains a similar reaction profile since it does not interact with the ${}^2A'$ states. The ${}^2A'$ states, on the other hand, will undergo typical configuration mixing, and as a result the two channels PT1 and PT2 also mix. Namely, both products, $\text{C}_2\text{H}(\Sigma^+)$ and $\text{C}_2\text{H}(\Pi)$, can be formed from either reactants $\text{NH}_3 + \text{C}_2\text{H}_2^+$ or $\text{NH}_3^+ + \text{C}_2\text{H}_2$, a typical nonadiabatic scenario. In addition, we have located a ${}^2A'$ transition state structure in C_s , **PT_TS2** as shown in Fig. 1. Judging solely from the structure and the normal mode also presented in Fig. 1, one may presume that this is a proton transfer transition state like **PT_TS1**. Since this conjecture does not agree with other calculation results just discussed, we have carried out intrin-

sic reaction coordinate (IRC) calculations to examine the nature of this structure. Interestingly, IRC indicates that **PT_TS2** actually connects intermediate **PT_1** and **CC_1**, a covalent NH_3CHCH^+ complex which shall be discussed later. The scanned potential energy surfaces which will be discussed in the section dealing with CT also support this result. Therefore, the PT channel and the covalent complex channel are now connected via **PT_TS2** which is only 0.30 eV above **PT_1** at the G2M/B3PW91/6-311G(*d,p*) level.

B. Covalent $\text{C}_2\text{H}_5\text{N}^+$ complex formation channel

For the system of $\text{C}_2\text{H}_5\text{N}^+$, there are a few known isomers from experiment work as well as theoretical calculations.⁴ In the work of Bouchoux *et al.*,⁴ the structures of three isomers and the transition states connecting them have been obtained at the MP2/6-31G(*d,p*) level. These results have been confirmed in the current work by the B3PW91/6-311G(*d,p*) method, and correspond to the structures **CC_2** ($\text{NH}_2\text{CHCH}_2^+$), **CC_3** (NHCHCH_3^+) and **CC_4** ($\text{NH}_2\text{CCH}_3^+$), and **CC_TS_23**, **CC_TS_24** and **CC_TS_34**, as presented in Fig. 4. Their relationships can be visualized more clearly in the schematic potential profile presented in Fig. 2. The agreement in both the geometrical

parameters and relative energetics between the current and previous calculations is good. Since this part of the potential energy surfaces has already been discussed in the previous work, we will not discuss much in detail except noting a few points. First of all, the most stable isomer **CC_2** ($\text{NH}_2\text{CHCH}_2^+$) is in a ${}^2A''$ state, with the electronic configuration of $(\pi)^2(\pi_n)^1$. Therefore, the ${}^2A'$ state corresponding to $\sigma \rightarrow \pi_n$ excitation from this state must be very high in energy, while the ${}^2A''$ state of $\pi \rightarrow \pi_n$ character might be relatively low lying. The reason for mentioning the electronic excited state will become clear in a moment. The intermediates **CC_3** and **CC_4** are both in the ${}^2A'$ state, and have the electronic configuration of $(\pi_{\text{N-C}})^2(n_{\text{N}})^1$ and $(\pi_{\text{N-C}})^2(n_{\text{C}})^1$, respectively. As a result, the C–N bond in **CC_3** and **CC_4** have larger double bond character and shorter distances than the C–N bond in **CC_2**. It is expected that the ${}^2A''$ excited states for **CC_3** and **CC_4** are of $\pi \rightarrow n$ nature and should be relatively low in energy compared to the ${}^2A'$ excited states. Judging from the symmetry of electronic states of these three complexes, one might expect that the transition states connecting **CC_2** and **CC_3**, **CC_2** and **CC_4**, should adopt C_1 symmetry. The located transition state, **CC_TS_24**, indeed has a C_1 structure. The other saddle point, **CC_TS_23**, on the other hand, has a perfect C_s symmetry and has only one imaginary frequency (a') corresponding to the H-atom transfer from the N atom to the terminal C atom. This result is not contradictory to any symmetry rule, since one observes that the CH_2 group has rotated around the C–C bond in the transition state, namely the C–C π bond has already broken, which is exactly required during the transformation from **CC_2** to **CC_3**. Therefore, the character of **CC_TS_23** is correct for being the transition state connecting **CC_2** and **CC_3**, it just happens that the structure is C_s .

The intermediates **CC_2** to **CC_4** are not directly connected with the reactant of the current system $\text{NH}_3 + \text{C}_2\text{H}_2^+$. To fill this gap, we have searched for and obtained two isomers of structure NH_3CHCH^+ , **CC_1_cis/trans**, which seem to have been overlooked in the previous studies. As seen from Fig. 4, the complex is the product of NH_3^+ addition directly to C_2H_2 . The π system in the C_2H_2 is broken, and a C–N single bond is formed, with an unpaired electron left on the end C atom. Both *cis*- and *trans*- structures are quite stable and lie around 3.0 eV below the reactants of $\text{NH}_3 + \text{C}_2\text{H}_3^+$. The excited ${}^2A'$ state must be of $\pi_{\perp} \rightarrow \pi_{\perp}^*$ type, and is expected to be very high in energy. In contrast, the excited ${}^2A''$ state is expected to be of $\pi_{\perp} \rightarrow n_{\text{C}}$ nature, and should be relatively low in energy.

The saddle point that connects **CC_1** and the more stable structure **CC_2** has also been obtained, which is **CC_TS_12**, shown in Fig. 4. The structure of **CC_TS_12** is also perfectly C_s , and has only one imaginary frequency corresponding to the H-atom transfer. If the reaction proceeds in C_s , **CC_TS_12**, a ${}^2A'$ state, cannot produce **CC_2**, which is a ${}^2A''$ state. Keeping the symmetry of **CC_TS_12**, geometry optimization leads to a structure (not shown) similar to **CC_2**, but with the NH_2 group adopts the orientation like in **CC_TS_12**. As expected, this structure has all real a' frequencies but a large a'' imaginary fre-

quency, indicating that the arrangement of the NH_2 group in **CC_2** is much more favorable since a conjugate N–C–C π system is formed. In other words, bifurcation of the reaction path has to take place somewhere between **CC_TS_12** and **CC_2**. At the G2M//B3PW91/6-311G(*d,p*) level, **CC_TS_12** lies 1.31 eV below the reactants of $\text{NH}_3 + \text{C}_2\text{H}_2^+$, i.e., the height of the barrier connecting **CC_2** measured from **CC1_trans** is 1.60 eV.

Up to now, no entrance channel barrier has been found on the lowest adiabatic potential energy surface, which makes it even more mysterious that no products from the covalent $\text{C}_2\text{H}_5\text{N}^+$ complexes have been found in the experimental work.² To possibly understand this, one has to realize one delicate question: the covalent complexes **CC_1** to **CC_4** correlate to $\text{NH}_3 + \text{C}_2\text{H}_2^+$ or $\text{NH}_3^+ + \text{C}_2\text{H}_2$? In other words, does $\text{NH}_3 + \text{C}_2\text{H}_2^+$ produce these complexes in their electronic ground states, or in their electronic excited states? Adiabatically, this is determined by the relative energetics of the two reactant limits. As seen in Fig. 2, $\text{NH}_3^+ + \text{C}_2\text{H}_2$ at their equilibrium geometries are more stable than $\text{NH}_3 + \text{C}_2\text{H}_2^+$ by ~ 1.22 eV at the G2M level. However, we also note that NH_3 and NH_3^+ have very different equilibrium geometries, the former has a pyramidal structure, while the latter is planar and becomes destabilized strongly by the umbrella motion. Therefore, the relative stability of the two asymptotes, $\text{NH}_3^+ + \text{C}_2\text{H}_2$ and $\text{NH}_3 + \text{C}_2\text{H}_2^+$, is expected to be a sensitive function of the NH_3 geometry. The situation is illustrated in Fig. 5(a), where the relative energies of the two asymptotes¹⁶ are scanned at the level of RCCSD(T)/6-311G(*d,p*) as a function of the ‘‘umbrella angle’’ $\angle \text{XNH}$, with X a dummy along the C_{3v} axis of NH_3 . The value of the $\angle \text{XNH}$ is 113.03° in the equilibrium NH_3 , and 90.0° in the equilibrium NH_3^+ . It is seen that even at the equilibrium structures of NH_3 , the reactants in the experiment, $\text{NH}_3 + \text{C}_2\text{H}_2^+$ are still higher in energy than $\text{NH}_3^+ + \text{C}_2\text{H}_2$ by ~ 0.5 eV. Therefore, it is most likely that the $\text{NH}_3 + \text{C}_2\text{H}_2^+$ will adiabatically correlate to excited states of these covalent $\text{C}_2\text{H}_5\text{N}^+$ species. In addition, it is also seen that the energy of the two asymptotes crosses when $\angle \text{XNH}$ is just 4° larger than that in equilibrium NH_3 , which suggests an efficient charge-transfer process with favorable Frank–Condon overlap at a long range. Indeed, CT is the most dominant process in all collision energies in the experiment of Anderson *et al.*²

Since we conclude that $\text{NH}_3 + \text{C}_2\text{H}_2^+$ should adiabatically correlate to excited states of the covalent complexes, we have carried out additional calculations for these species, and the resultant structures labeled with ‘‘ex’’ (stands for excited state) have also been included in Fig. 4. According to the electronic configuration analysis mentioned in the discussion above, we see that for all the covalent complexes **CC_1** to **CC_4**, the ${}^2A'$ excited states are all expected to be very high in energy, while the ${}^2A''$ excited states should be relatively low lying. Therefore, only ${}^2A''$ excited states have been calculated in the current work. For **CC_3**, **CC_4**, and **CC_1**, the ground electronic states are ${}^2A'$, and therefore the ${}^2A''$ excited states can be obtained at the B3PW91 level by altering orbital occupation patterns. For **CC_2**, two structures with different NH_2 orientations have been investigated, which are **CC_2_ex** and **CC_2_ex2** in Fig. 4. Since, with

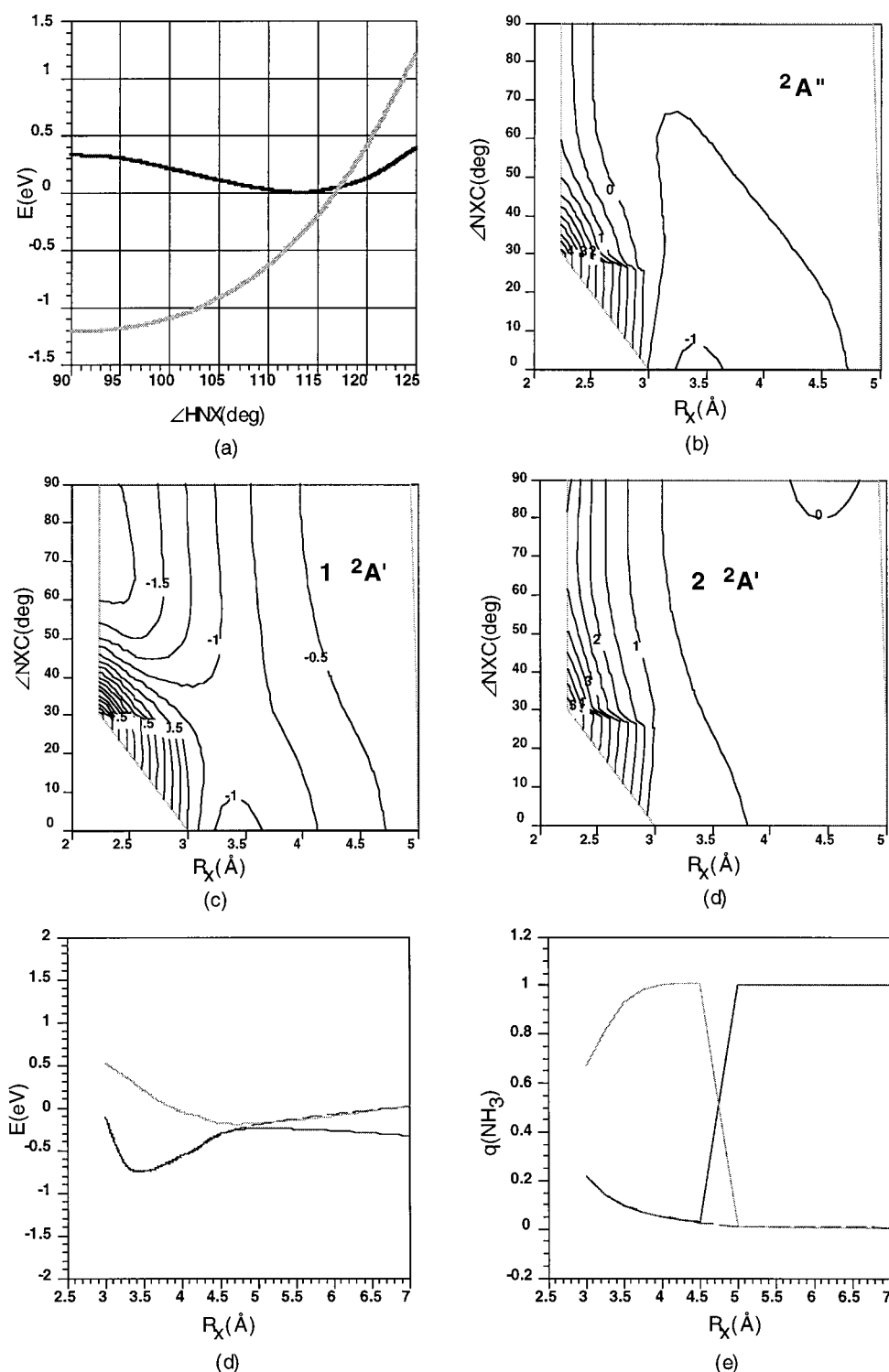


FIG. 5. (a) Energies (in eV) of the two asymptotes $\text{NH}_3 + \text{C}_2\text{H}_2^+$ and $\text{NH}_3^+ + \text{C}_2\text{H}_2$ as a function of the umbrella motion, which is characterized by the $\angle\text{HNX}$ (in deg, see text for details). (b)–(d) Contour plots (in eV) for the potential energy surface related to the charge-transfer channel scanned at the CASSCF(5e/5o)/6-31G(d,p) level. The electronic states have been labeled in the figures. $\angle\text{HNX}$ is fixed at 110.0° . (e)–(f) Potential energy (in eV) and charge population on the NH_3 fragment of the three electronic states (1, $2^2A'$ and $2^2A''$) as a function of R_{NX} (in \AA) upon collinear approach. $\angle\text{NHX}$ is fixed at 110.0° .

the conformation of the **CC_2_ex_2**, the ground state is $2^2A''$ and therefore its $2^2A''$ excited states have to be calculated by methods other than DFT, and the EOM-CCSD/6-311G(d,p)//EOM-CCSD/6-31G(d,p) method has been chosen in the current work. For structure **CC_2_ex**, on the

other hand, the B3PW91 method has been used.

As seen in Fig. 4, the geometries of the excited state structures for the covalent species reflect clearly the change of electronic configurations compared to the ground electronic states discussed above. For instance, the C–N dis-

tances have stretched significantly in both **CC_3_ex** and **CC_4_ex** compared to those in their ground electronic states, due to the excitation of $\pi \rightarrow n$. Similarly, the C–C distance in **CC_1_ex** is also stretched from that in **CC_1**. For the excited state of **CC_2**, it is interesting to note that even though the NH_2 group prefers to be in the N–C–C plane in **CC_2**, the structure with NH_2 perpendicular to the N–C–C plane, **CC_2_ex**, is much more stable than **CC_2_ex_2** in the excited state by nearly 2.3 eV. Evidently, the lone pair on NH_2 prefers to be decoupled from the C–C π system in the excited state. Therefore, even without frequency analysis for **CO_2_ex_2** at the EOM-CCSD level, we expect that it has one imaginary frequency. Energetically, **CC_1_ex**, **CC_3_ex**, **CC_2_ex** are all below the reactants of $\text{NH}_3 + \text{C}_2\text{H}_2^+$, while **CC_4_ex** is 0.10 eV above $\text{NH}_3 + \text{C}_2\text{H}_2^+$.

Furthermore, we have also calculated a few transition states on the $^2A''$ electronic state, where attention has been mainly focused on the entrance barrier and the isomerization barrier between **CC_1_ex** and **CC_2_ex**. We hope that the entrance and isomerization barriers on the $^2A''$ excited states will be high in energy, so that $\text{NH}_3 + \text{C}_2\text{H}_2^+$ shall mainly follow other paths such as CT and PT, and the experimental results can then be rationalized to some extent. Unfortunately, the two transition states we have obtained here at the G2M/B3PW91/6-311G(*d,p*) level are not high in energy at all, but rather close to the reactants. More specifically, **CC_TS_ex**, a saddle point with long N–C distance of 1.97 Å, is found to be 0.05 eV above the reactants when ZPE is included in the G2M values, and the isomerization transition state between **CC_1_ex** and **CC_2_ex_2** i.e., structure **CC_TS_12_ex**, is 0.02 eV below $\text{NH}_3 + \text{C}_2\text{H}_2^+$. Since the energy of **CC_TS_ex** is lower than the reactants at the B3PW91/6-311G(*d,p*) level, we have also tried to locate a long-range complex between NH_3 and C_2H_2^+ . However, all attempts lead to the stable complex involved in the PT channel, **PT_1**. Therefore, **CC_TS_ex** might be better described as the transition state connecting **PT_1** and **CC_1_ex**, the $^2A''$ correspondence of **PT_TS2** in the $^2A'$ symmetry. Nevertheless, the energetics of **CC_TS_ex** indicates that the long-range potential of the $^2A''$ state is rather attractive and no large barrier is expected.

In short, we have found no barriers on either the ground or the $^2A''$ excited electronic states that are significantly high in energy compared to the reactants of $\text{NH}_3 + \text{C}_2\text{H}_2^+$. In fact, all the structures here even in the $^2A''$ excited states are below 0.1 eV (the lowest collision energy in the experiment) relative to $\text{NH}_3 + \text{C}_2\text{H}_2^+$. Although we might argue that PT and CT are more efficient due to the large exothermicity in the former channel and the favorable FC overlap at long range for the latter, it is hard to believe that no covalent $\text{C}_2\text{H}_5\text{N}^+$ will be accessed at all. Furthermore, since $\text{NH}_3^+ + \text{C}_2\text{H}_2$ correlates to the ground state of these covalent species, it seems reasonable to expect that some covalent $\text{C}_2\text{H}_5\text{H}^+$ will be formed after the CT process, especially at low collision energy ~ 0.1 eV. Evidently, the experimental results that no product from the covalent $\text{C}_2\text{H}_5\text{H}^+$ formation channel has been observed at all still remains a mystery and

requires further theoretical as well as experimental investigation.

C. Charge-transfer channel (CT)

Among the three channels, the charge-transfer process is the most difficult to characterize due to its lacking the capability of pinning down a minimum on the seam of crossing (MSX) structures for states of same symmetry with highly correlated methods. Therefore, our goal here is to obtain some qualitative feature of the potential energy surfaces that can be used to analyze the experimental findings. First of all, we recall from the previous section that the two reactant limits, $\text{NH}_3 + \text{C}_2\text{H}_2^+$ and $\text{NH}_3^+ + \text{C}_2\text{H}_2$ are very close in energy, especially with minor excitation of the NH_3 umbrella mode. Therefore, a favorable FC overlap is expected at long range, which suggests an efficient long-range electron transfer process, as observed in the experiment.

We have carried out potential energy surface scans for the three electronic states involved in the CT channel to examine the qualitative feature of the potentials when the two fragments NH_3^+ and C_2H_2^+ interact. For the scans, a three-state-averaged (two $^2A' + ^2A''$) CASSCF calculation has been performed. The active space for five electrons in five orbitals in the CASSCF calculation includes the $\pi_{\parallel,\perp}$ and $\pi_{\parallel,\perp}^*$ orbitals on C_2H_2^+ and the lone pair on the NH_3 . The C_2H_2 part has been fixed at its equilibrium structure obtained at the CASSCF/6-31G(*d,p*) level, and the H–N distance in the NH_3 has been fixed to be 1.0 Å. This leaves three degrees of freedom: R_X , the distance between N and the center of mass of C_2H_2 ; $\angle NXC$, the angle that describes the relative orientations of NH_3 and C_2H_2 and will be referred to as “approaching angles” in the later discussion; and the $\angle HNX$ which characterizes the umbrella motion of the NH_3 , the same as defined previously. Selected contour plots of energies at fixed $\angle HNX$ are shown in Figs. 5(b)–5(d).

The contour plots in Figs. 5(b)–5(d) show the qualitative feature of the three adiabatic potentials as functions of R_{NX} and $\angle NXC$ with $\angle HNX$ fixed at 110° . The shape of the $^2A''$ state shown in Fig. 5(b) is rather simple and coincides with expectation. There is one potential well along the linear approach of NH_3 toward C_2H_2^+ , which is expected to lead to the minimum **PT_1** upon further C–H stretch. The potential energy surface is repulsive for large angle approaches, which is consistent with the fact that the lone pair on NH_3 disfavors the π_{\parallel} of $^2A''$ C_2H_2^+ . The shape of the $1^2A'$ state is quite interesting, as shown in Fig. 5(c), and confirms many findings mentioned during the previous discussion on the PT channels. At linear approach, the potential well is of the same character as the one on the $^2A''$ surface. It should be emphasized once again that this well on the $1^2A'$ adiabatic surface can correlate to the reaction limit of $\text{NH}_3^+ + \text{C}_2\text{H}_2$ as well for nonlinear configurations due to nonadiabatic interactions. Upon approaching 60° for $\angle NXC$, there is another deeper minimum which is related to **CC_1**. Between the two wells is a saddle point, which corresponds to the structure **PT_TS2**. The shape of the $2^2A'$ surface is repulsive for all the approaching angles, which manifests the strong interaction between the two $^2A'$ states.

It is interesting to notice the unique situation where the two fragments approach with small angles or collinearly. In this case, the configuration mixing between the two ${}^2A'$ states is smaller due to the fact that they belong to different irrep. 2A_1 and 2E , respectively, in exact collinear case. Therefore, the potential curves of the three electronic states, $1,2{}^2A'$ and ${}^2A''$ may stay rather close up to a weakly avoided crossing, as illustrated in Fig. 5(e). The change of the electron population on the NH_3 fragment is also shown as a function of R_{NX} in Fig. 5(f). Clearly, the switching for the character of the two A' states is rather sudden.

D. Relationship to experiment

Based on the findings we have discussed above, we can make a few comments on the experimental observations. First of all, both two-proton transfer channels (actually hydrogen atom transfer in the PT2 channel) are expected to proceed rather easily due to the low energies of the intermediates and transition states involved, which is consistent with the “stripping” mechanism proposed by Anderson *et al.*²

With the information from the current study, the mystery that no product from the covalent complex formation channel has been observed in the experiment, can be rationalized to some extent. We argue that $\text{NH}_3 + \text{C}_2\text{H}_2^+$ correlates to the excited states of the low lying covalent $\text{C}_2\text{H}_5\text{N}^+$ complexes, and most likely to sample the $2{}^2A'$ and ${}^2A''$ surface. As we have seen in Secs. III B and III C, the $2{}^2A'$ surface is repulsive for all the approaching angles, and therefore reaction is not expected to take place on this state. Although no barrier significantly high in energy has been found in Sec. III B, the ${}^2A''$ surface is repulsive for most approaching angles with fixed C_2H_2 , but is attractive for the collinear arrangement of $\text{NH}_3 \cdots \text{C}_2\text{H}_2^+$. Therefore, the system is most likely to follow to PT channel, since significant alternation is the geometry and electronic configuration of C_2H_2^+ is required to lower the energy of the path leading to the covalent $\text{C}_2\text{H}_5\text{N}^+$ complexes in their ${}^2A''$ excited states. In fact, we expect that the complex formation channel is more likely to be accessed if H–C–C bending as well as C–C stretch are excited in the reactant C_2H_2^+ .

The fact that no H-abstraction products $\text{NH}_2 + \text{C}_2\text{H}_3^+$ have been observed experimentally can be understood in a similar fashion, albeit without any calculation. Even the ground state products of this channel are endothermic by 0.14 eV at the G2M//B3PW91/6-311G(*d,p*) level, and therefore the excited state products that correlate to $\text{NH}_2 + \text{C}_2\text{H}_3^+$ are expected to be very high in energy. Consequently, it is not surprising that the channel was not observed experimentally.

As to the charge-transfer process, two pathways seem to exist according to the different product recoil velocity distribution.² Although it is not totally clear from the current study what these two paths are, one may make some speculation. First of all, one may imagine different crossing structures depending on the approaching angles of the two fragments. As we have seen in Sec. III C, the two asymptotes, $\text{NH}_3 + \text{C}_2\text{H}_2^+$ and $\text{NH}_3^+ + \text{C}_2\text{H}_2$, are rather close in energy at the $\text{NH}_3 + \text{C}_2\text{H}_2^+$ geometry. As the two fragments NH_3^+ and

C_2H_2^+ approach with large angles, the two ${}^2A'$ states interact strongly and the $2{}^2A'$ adiabatic state becomes repulsive. Therefore, there exists a good chance of the potential energy surface to cross at long separation. The charge transfer cannot take place at very far nuclear separation, however, due to the weak interaction between the electronic states and therefore a small coupling element. Consequently, to have a good Franck–Condon factor as well as a reasonably large coupling element, an intermediate range crossing structure is desired. On the other hand, the situation is rather different when the two fragments approach with small angles close enough to be linear. In this case, the two ${}^2A'$ surfaces interact rather weakly due to their diabatic characters and undergo weakly avoided crossings. As a result, the CT channel in the linear configuration case might yield products of quite different characteristics. In addition, one may also suspect that the two charge-transfer paths come from different nonadiabatic processes, namely $A' \rightarrow A'$ CT and $A'' \rightarrow A'$ CT, respectively. To have more quantitative results, one needs to optimize the MSX structures for ${}^2A'/{}^2A'$, and also ${}^2A'/{}^2A''$, probably as a function of relative approaching angle of the fragments. These calculations have not been carried out in the current study.

Clearly, more elaborate work on the CT channel and possibly the excited states of the covalent complexes have to be carried out to further understand the experimental results of Anderson *et al.*² In particular, we are still puzzled as to why no products from the covalent complex channel have been observed *at all*. Even these low lying complexes correlate adiabatically with the $\text{NH}_3^+ + \text{C}_2\text{H}_2$, and the CT and PT processes are very efficient; one may imagine that some amount, if not much, of a complex like **CC_1** can be produced either on the ${}^2A''$ excited state directly, or on the ground electronic state after the charge transfer has occurred.

IV. CONCLUSIONS

High level *ab initio* calculations have been carried out to study the mechanism of the ion–molecule reaction $\text{NH}_3 + \text{C}_2\text{H}_2^+$. Three channels, covalent complex formation, proton transfer (PT) and charge transfer (CT) have been studied, and the findings can be summarized as the following:

- (1) Two PT channels have been characterized. In C_{3v} symmetry where the N–C–C framework is linear, the reactants $\text{NH}_3 + \text{C}_2\text{H}_2^+$ lead to the proton transfer products $\text{NH}_4^+ + \text{C}_2\text{H}({}^2\Pi)$. While $\text{NH}_3^+ + \text{C}_2\text{H}_2$ leads to the H-atom transferred products $\text{NH}_4^+ + \text{C}_2\text{H}({}^2\Sigma^+)$. The former process proceeds without any barrier, and only through a moderately bound complex which is much productlike. The later process, however, proceeds with a barrier but without any intermediate. On the $1{}^2A$ state surface, we have also located a transition state that connects the intermediates in the first PT channel to the covalent species **CC_1**. These findings support the fast “stripping” mechanism proposed by Anderson *et al.* based on their experimental results.
- (2) Although the $2{}^2A'$ excited state of $\text{C}_2\text{H}_5\text{H}^+$ is expected to be high in energy, no significant barrier compared to

the reactants has been found on either the ground or the ${}^2A''$ excited state surfaces. Several isomers of $C_2H_5N^+$, **CC_1-4**, and the isomerization transition states between them have been located, and the results for the ground electronic state structures agree well with previous studies. To rationalize the experimental fact that no covalent complex channel products have been observed, we argue that the reactants $NH_3+C_2H_2^+$ correlate adiabatically to the excited states of these covalent $C_2H_5N^+$ species. Although not very high in energy, the formation of these complexes requires significant alternation of the $C_2H_2^+$ geometry and electronic structure. Therefore, the system is most likely to follow the PT channel instead of visiting the covalent complex formation channel. However, the experimental fact that no products from the covalent complexes have been observed still remains a mystery. The fact that no H-abstraction products $NH_2+C_2H_3^+$ have been observed can be understood in a similar fashion, although no calculations have been carried out in the current work.

- (3) For the CT channel, only limited potential energy surface scans have been carried out to study the qualitative feature of the three electronic states ($1,2\ {}^2A'+{}^2A''$). It was found that the ${}^2A''$ state is repulsive in most regions except around linear configuration, where the potential energy is attractive and readily leads to CT or PT. The shape of the $1\ {}^2A'$ state confirms the existence of a saddle point between the potential well at the linear configuration and **CC_1**, which has been optimized as **PT_TS2**. The $2\ {}^2A'$ state is mostly repulsive at all approaching angles. Charge transfer at different approaching angles, or CT between electronic states of different symmetries, ($A' \rightarrow A'$, $A'' \rightarrow A'$) may produce final products of different characteristics, and might account for the two pathways proposed by Anderson *et al.*² based on the different product recoil distributions.

To further understand the experimental observations, more elaborate calculations are required, particularly on the MSX structures between the three electronic states, which will be pursued in the near future.

ACKNOWLEDGMENTS

The authors would like to acknowledge Dr. Scott Anderson for experimental results prior to publication and for stimulating discussions. Q.C. acknowledges a graduate fellowship from the Phillips Petroleum Co. This work was in part supported by the Grant No. F49620-95-1-0182 from the Air Force Office of Scientific Research.

- ¹(a) A. Luna, A. M. Mebel, and K. Morokuma, *J. Chem. Phys.* **105**, 3187 (1996); (b) A. M. Mebel, A. Luna, M. C. Lin, and K. Morokuma, *ibid.* **105**, 6439 (1996).
- ²J. Qian, H. Fu, and S. L. Anderson, *J. Phys. Chem.* (submitted).
- ³(a) Y. Chiu, H. Fu, J. Huang, and S. L. Anderson, *J. Chem. Phys.* **102**, 1119 (1995); (b) **101**, 5410 (1994); (c) R. D. Guettler, G. C. Jones, Jr., L. A. Posey, and R. N. Zare, *Science* **266**, 259 (1994).
- ⁴G. Bouchoux, F. Penaud-Berruyer, and M. T. Nguyen, *J. Am. Chem. Soc.* **115**, 9728 (1993).
- ⁵(a) A. D. Becke, *Phys. Rev. A* **38**, 3098 (1988); (b) C. Lee, C. Yang, R. G. Parr, *Phys. Rev. B* **37**, 785 (1988); (c) A. D. Becke, *J. Chem. Phys.* **98**, 5648 (1993).
- ⁶(a) J. P. Perdew and Y. Wang, *Phys. Rev. B* **34**, 13244 (1992); (b) A. D. Becke, *J. Chem. Phys.* **97**, 9173 (1992).
- ⁷R. Krishnan, J. S. Binkley, R. Seeger, and J. A. Pople, *J. Chem. Phys.* **72**, 650 (1980).
- ⁸A. M. Mebel, K. Morokuma, and M. C. Lin, *J. Chem. Phys.* **103**, 7414 (1995).
- ⁹See, for example, H.-J. Werner, *Adv. Chem. Phys.* **69**, (1987).
- ¹⁰P. C. Hariharan and J. A. Pople, *Theor. Chim. Acta* **28**, 213 (1973).
- ¹¹Q. Cui, Z. Liu, and K. Morokuma, *J. Chem. Phys.* (submitted).
- ¹²GAUSSIAN94, Revision D.3. M. J. Frisch, G. W. Trucks, H. B. Schlegel, P. M. W. Gill, B. G. Johnson, M. A. Robb, J. R. Cheeseman, T. Keith, G. A. Petersson, J. A. Montgomery, K. Raghavachari, M. A. Al-Laham, V. G. Zakrzewski, J. V. Ortiz, J. B. Foresman, J. B. Cioslowski, B. Stefanov, A. Nanayakkara, M. Challacombe, C. Y. Peng, P. Y. Ayala, W. Chen, M. W. Wong, J. L. Andres, E. S. Replogle, R. Gomperts, R. L. Martin, D. J. Fox, J. S. Binkley, D. J. Defrees, J. Baker, J. P. Stewart, M. Head-Gordon, C. Gonzalez, and J. A. Pople, Gaussian, Inc., Pittsburgh, PA, 1995.
- ¹³MOLPRO96, P. J. Knowles and H.-J. Werner, University of Birmingham, 1996.
- ¹⁴See, for example, Y.-C. Hsu, Y.-J. Shiu, and C.-M. Lin, *J. Chem. Phys.* **103**, 5919 (1995).
- ¹⁵See for example, M. Peric, W. Reuter, and S. D. Peyerimhoff, *J. Mol. Spectrosc.* **148**, 201 (1991), and references therein.
- ¹⁶The potential curve of NH_3^+ has been shifted according to the (0,0) separation of the two asymptotes obtained with experimental data for the I.P. of C_2H_2 and NH_3 .